Soil Biology & Biochemistry 111 (2017) 143–153

Contents lists available at ScienceDirect

Soil Biology & Biochemistry

journal homepage: www.elsevier.com/locate/soilbio

Nitrification gene ratio and free ammonia explain nitrite and nitrous oxide production in urea-amended soils

Florence Breuillin-Sessoms [a], Rodney T. Venterea [b, c, *], Michael J. Sadowsky [a, b], Jeffrey A. Coulter [d], Tim J. Clough [e], Pang Wang [a]

[a] Biotechnology Institute, Univ. of Minnesota, St. Paul, MN, 55108, USA
[b] Dept. of Soil, Water & Climate, Univ. of Minnesota, St. Paul, MN, 55108, USA
[c] USDA-ARS, Soil & Water Management Research Unit, St. Paul, MN, 55108, USA
[d] Dept. of Agronomy & Plant Genetics, Univ. of Minnesota, St. Paul, MN, 55108, USA
[e] Faculty of Agriculture & Life Sciences, Lincoln Univ., P.O. Box 85084, Lincoln, 7647, Canterbury, New Zealand

ARTICLE INFO

Article history:
Received 1 December 2016
Received in revised form
27 March 2017
Accepted 5 April 2017

ABSTRACT

The atmospheric concentration of nitrous oxide (N_2O), a potent greenhouse gas and ozone-depleting chemical, continues to increase, due largely to the application of nitrogen (N) fertilizers. While nitrite (NO_2^-) is a central regulator of N_2O production in soil, NO_2^- and N_2O responses to fertilizer addition rates cannot be readily predicted. Our objective was to determine if quantification of multiple chemical variables and structural genes associated with ammonia (NH_3)- (AOB, encoded by *amo*A) and NO_2^--oxidizing bacteria (NOB, encoded by *nxr*A and *nxr*B) could explain the contrasting responses of eight agricultural soils to five rates of urea addition in aerobic microcosms. Significant differences in NO_2^- accumulation and N_2O production by soil type could not be explained by initial soil properties. Biologically-coherent statistical models, however, accounted for 70–89% of the total variance in NO_2^- and N_2O. Free NH_3 concentration accounted for 50–85% of the variance in NO_2^- which, in turn, explained 62–82% of the variance in N_2O. By itself, the time-integrated *nxr*A:*amo*A gene ratio explained 78 and 79% of the variance in cumulative NO_2^- and N_2O, respectively. In all soils, *nxr*A abundances declined above critical urea addition rates, indicating a consistent pattern of suppression of *Nitrobacter*-associated NOB due to NH_3 toxicity. In contrast, *Nitrospira*-associated *nxr*B abundances exhibited a broader range of responses, and showed that long-term management practices (e.g., tillage) can induce a shift in dominant NOB populations which subsequently impacts NO_2^- accumulation and N_2O production. These results highlight the challenges of predicting NO_2^- and N_2O responses based solely on static soil properties, and suggest that models that account for dynamic processes following N addition are ultimately needed. The relationships found here provide a basis for incorporating the relevant biological and chemical processes into N cycling and N_2O emissions models.

Published by Elsevier Ltd.

1. Introduction

Nitrous oxide (N_2O) has two important ecological impacts; it is the predominate ozone-depleting chemical (Ravishankara et al., 2009) and a potent greenhouse gas (Forster et al., 2007) that has increased in atmospheric concentration by more than 20% since 1750, due largely to the application of N fertilizers and manures (Davidson, 2009; Ciais et al., 2013). It is estimated that 3–5% of anthropogenic nitrogen (N) inputs applied to agricultural ecosystems are eventually emitted to the atmosphere as N_2O (Crutzen et al., 2008). Thus, there is much interest in quantifying the effects of nitrogen (N) fertilizer inputs on soil-to-atmosphere N_2O emissions. In particular, substantial efforts have been made to characterize the functional responses (e.g., linear vs. non-linear) of N_2O emissions to N fertilizer addition rates (Shcherbak et al., 2014). Such responses can be used to parameterize N_2O emission models (Zhou et al., 2015). It is generally understood that an imbalance between N fertilizer inputs and plant N uptake capacity promote N_2O losses, due in large part to elevated soil inorganic N availability, which in turn enhances soil microbial processes including

* Corresponding author. USDA-ARS, Soil & Water Management Research Unit, St. Paul, MN, 55108, USA.
E-mail address: Venterea@umn.edu (R.T. Venterea).

http://dx.doi.org/10.1016/j.soilbio.2017.04.007
0038-0717/Published by Elsevier Ltd.

nitrification and denitrification. Both of these processes can lead to gaseous emissions of N_2O, ammonia (NH_3) and nitric oxide (NO), and also regulate nitrate (NO_3^-) leaching to ground and surface waters (Firestone and Davidson, 1989; Robertson and Vitousek, 2009). While it is well known that soil processes interact with plant and climatic factors to regulate N_2O emissions (Venterea et al., 2012), few studies have simultaneously quantified multiple chemical variables and genetic markers of specific soil microbial processes following N fertilizer addition.

Production of N_2O in soil can occur via chemo-denitrification (Stevenson et al., 1970), bacterial heterotrophic denitrification (Zumft, 1997) and nitrifier-denitrification (Wrage et al., 2001). In all of these processes, nitrite (NO_2^-) serves as a proximal substrate for N_2O production. Although soil NO_2^- concentrations are commonly low compared to ammonium (NH_4^+) and NO_3^-, even low NO_2^- concentrations can be important due to rapid N_2O production kinetics (Venterea, 2007). Moreover, due to its role as a central substrate in these multiple N cycling processes, NO_2^- concentrations correlate better with N_2O emissions than either NH_4^+ or NO_3^- concentrations under field (Venterea and Rolston, 2000; Maharjan and Venterea, 2013) and laboratory (Ma et al., 2015; Cai et al., 2016) conditions. Accurate determination of soil NO_2^- concentrations requires careful consideration with regard to methods of sampling, storage, extraction, and analysis (Stevens and Laughlin, 1995; Maharjan and Venterea, 2013; Homyak et al., 2015).

Nitrite can be produced and consumed both aerobically, via nitrification, and anaerobically via denitrification (Burns et al., 1996). In the days to weeks following application of urea, the accumulation of NO_2^- is mainly regulated by nitrification, even in the presence of NO_3^- and over a range of soil water contents (Van Cleemput and Samater, 1995; Smith et al., 1997; Shen et al., 2003). Nitrification is generally considered to be a two-step process, wherein NH_3 is first oxidized to NO_2^- by ammonia-oxidizing bacteria (AOB) and/or archaea (AOA), followed by the oxidation of NO_2^- to NO_3^- by nitrite-oxidizing bacteria (NOB) (Heil et al., 2016). Recently, some NOB within the genus *Nitrospira* have been found to be capable of oxidizing both NH_4^+ and NO_2^- (Daims et al., 2015; van Kessel et al., 2015), although the prevalence of bacteria with this metabolic capability, referred to as "complete nitrification" or "comammox," in agricultural soils is unknown. While the two steps of nitrification are often tightly coupled, both temporally and spatially, the presence of free NH_3 can promote their decoupling, wherein NH_3 inhibits NOB such that the NO_2^- generated by NH_3 oxidation cannot be immediately processed and therefore accumulates (Stojanovic and Alexander, 1958; Smith et al., 1997; Park and Bae, 2009).

Because elevated pH favors NH_3 in its equilibrium with NH_4^+, initial soil pH is often considered an indicator of the soil NO_2^- accumulation potential (Shen et al., 2003). However, Venterea et al. (2015) observed that soil pH, and other basic soil properties including texture and carbon content, did not explain highly contrasting NO_2^- and N_2O production in two soils amended with urine or urea. In that study, greater accumulation of NO_2^- was associated with greater abundances of the *amo*A gene that encodes for ammonia monooxygenase in AOB, and lower abundances of the *nxr*A gene that encodes for nitrite oxidoreductase in *Nitrobacter*-associated NOB, while abundances of *amo*A that encodes for ammonia monooxygenase in AOA did not explain any of the variation. Venterea et al. (2015) also found that reductions in *nxr*A gene abundances were associated with increased free NH_3 concentrations which accounted for differences in soil NH_4^+ sorption capacity (ASC). Few, if any, studies have examined relationships among AOB- and NOB- gene copies, NH_3, NO_2^- and N_2O in N-amended soils. Improved understanding of NOB response to land management has recently been identified as an important research need (Koch et al., 2015; Bertagnolli et al., 2016; Daims et al., 2016). Quantification of the relative responses of *Nitrobacter* and *Nitrospira*, the two major NOB genera considered important in soil, has been facilitated by the development of polymerase chain reaction (PCR) primers that target the *nxr*A genes of *Nitrobacter* (Wertz et al., 2008) and, more recently, the *nxr*B genes of *Nitrospira* (Pester et al., 2014).

Consistent with Venterea et al. (2015), several recent studies have found that AOB are the dominant regulators of nitrification and N_2O production in non-acidic soils receiving N inputs equivalent to fertilizer or urine deposition rates (Di et al., 2009; Wertz et al., 2012; Chen et al., 2013; Banning et al., 2015; Giguere et al., 2015; Sterngren et al., 2015; Wang et al., 2016). In contrast, AOA have been found to be more important relative to AOB in acid soils (Prosser and Nicol, 2012; Shen et al., 2012; Zhang et al., 2012). Some studies have shown AOA to be important in regulating nitrification in non-acid soils amended with manure (Schauss et al., 2009), wastewater biosolids (Kelly et al., 2011), or relatively low concentrations ($\leq$50 μg N g^{-1} soil) of inorganic N (Giguere et al., 2017). Based on the large number of studies, cited above, indicating the likely importance of AOB in non-acidic soils receiving larger N inputs, the current investigation focused on quantifying AOB-associated *amo*A, together with NOB-associated *nxr*A and *nxr*B, in several non-acidic, urea-amended agricultural soils.

While the major processes regulating soil NO_2^- production are largely understood, NO_2^- dynamics, and associated N_2O production, for any given soil and management regime cannot be predicted. It is expected that NO_2^- and N_2O production will increase with increasing N input, but neither the magnitude nor functional nature of the responses to N addition rate have been well-characterized across a variety of soils. Our objective was to determine if simultaneous measurement of multiple chemical variables (NH_4^+, NH_3, NO_2^-, NO_3^-, N_2O and pH) and gene copy numbers of *amo*A, *nxr*A and *nxr*B could be used to elucidate controls over NO_2^- and N_2O production in eight agricultural soils following urea addition in aerobically incubated microcosms. We hypothesized that responses would vary widely across individual soil types and that the variation in these responses would be explained by a combination of these chemical and genetic variables, including the *nxr*A:*amo*A and *nxr*B:*amo*A gene ratios, which to our knowledge have not been evaluated previously.

2. Material and methods

2.1. Soil collection and characterization

Eight agricultural soils were collected from the University of Minnesota Research and Outreach Centers distributed geographically across the state. These sites included Becker (B), Crookston (C), Lamberton (L), Rosemount (R), St. Paul (S) and Waseca (W), representing a range of soil types used for crop production in the state (Table 1). Soil samples were collected following crop harvest in fall 2014 from the upper 0.15 m of plots that received no N fertilizer during the previous growing season. At Rosemount, two soils were collected from plots that had been under contrasting long-term tillage management since 1990, either conventional (soil R-CT) or no tillage (soil R-NT) (Venterea et al., 2006). All other soils were managed with conventional tillage practices for the region. At St. Paul, two soils were collected from plots that have been under contrasting crop management, either continuous corn (soil S-C) since 1975, or continuous soybean (soil S-S) since at least 1996. Samples were dried at room temperature for 7–10 d, ground, sieved (2 mm), homogenized, and stored at 4 °C prior to use in experiments.

Table 1
Properties of agricultural soils used in microcosm experiments.

	Units	Soil							
		B	C	L	W	R-CT	R-NT	S-C	S-S
Location		Becker 45.38° N 93.88° W	Crookston 47.80° N 96.61° W	Lamberton 44.23° N 95.30° W	Waseca 44.05° N 93.52° W	Rosemount 44.75° N 93.07°W	Rosemount 44.75° N 93.07°W	St. Paul 44.99° N 93.17° W	St. Paul 44.99° N 93.17° W
Cropping system[a]		Corn- *Soybean*	Soybean- *Wheat*	*Corn*- Soybean	*Corn*- Soybean	*Corn*-Soybean	*Corn*-Soybean	Corn	Soybean
Tillage		Disk/chisel				Moldboard	No till	Disk/chisel	
Soil series/ classification		Hubbard/Entic Hapludolls	Wheatville/Aeric Calciaquolls	Normania/Aquic Hapludolls	Webster/Typic Endoaquolls	Waukegan/Typic Hapludolls			
Texture class		Sandy loam	Loam	Clay loam	Clay loam	Silt loam	Silt loam	Silt loam	Silt loam
Clay	%	11.5	19.1	27.1	29.6	15.5	10.4	14.9	16.9
Silt	%	7.7	38.1	30.4	33.2	58.3	55.6	59.6	50.8
Sand	%	80.8	42.8	42.5	37.2	26.2	34.0	25.5	32.3
pH	1 M KCl	6.2	7.3	4.8	5.6	5.4	5.3	6.2	6.0
pH	H_2O	7.4	8.2	6.1	6.6	6.8	6.7	7.1	7.2
Organic matter[b]	%	4.5	3.6	6.5	8.4	5.0	7.0	5.9	3.4
Organic N[c]	g N kg^{-1}	0.93	1.73	1.67	2.39	1.74	2.29	2.11	1.15
Organic C	g C kg^{-1}	12.6	17.3[d]	17.8	30.2	22.3	28.6	25.1	15.3
CEC[e]	meq/ 100 g	8.1	44.3	19.6	36.7	20.1	21.2	20.4	16.2
K[f]	mg N L^{-1}	207	152	454	169	412	254	311	224
μ	μg N g^{-1}	642	1344	1960	1645	1743	1020	1269	949
Water content[g]	g H_2O g^{-1}	0.161	0.246	0.288	0.321	0.288	0.298	0.255	0.238

[a] For soils in two-year rotated cropping systems, the crop grown in the year of sample collection is shown in italics.
[b] Determined from loss on ignition at 450 °C for 16 h.
[c] Organic N and C determined by dry combustion using a VarioMax CN Macro Elemental Analyzer (Elementar, Langenselbold, Germany).
[d] This soil was acid-fumigated to remove carbonates prior to organic C analysis.
[e] Cation exchange capacity determined from sum of exchangeable cations using inductively coupled plasma atomic emission spectroscopy.
[f] Parameters K and μ from equation (1).
[g] Water content used in microcosms, equivalent to 85% of water-holding capacity.

2.2. Microcosm design and chemical analysis

Microcosm experiments were conducted using all eight soils. Ten to thirteen-g aliquots of air-dried soil were placed into 165 pre-sterilized 250-mL glass 'wide-mouth' jars. Soil in each jar was brought to a moisture content representing 85% of water-holding capacity by adding solutions containing reagent grade urea [$CO(NH_2)_2$] in purified water. For each soil, five treatment levels were established using initial urea concentrations of 0 (water only), 100, 250, 500, or 1000 μg N g^{-1} dry soil. These concentrations were chosen to represent a range of conditions following N fertilizer applications, including conditions within fertilizer bands and adjacent to dissolving urea granules (Wetselaar et al., 1972; Yadvinder-Singh and Beauchamp, 1989; Wang et al., 1998). Solutions were immediately mixed with soil for 20 s using a stainless steel spatula. The microcosms were designed to maintain aerobic conditions as previously described (Venterea et al., 2015). The soil occupied a thin (~3 mm) layer at the bottom of the jars, which were sealed for the majority of the incubation period. Jars were equilibrated with room air for 10 min on days 2, 10 and 24. This procedure minimized evaporative losses while maintaining headspace O_2 levels ≥18%, as confirmed by gas chromatographic analysis every 7–10 d.

Microcosms were incubated in the dark at 22 °C for 31 d, with sacrificial sampling of three replicate jars for each soil and urea level occurring 11 times at 3- or 4-d intervals (0, 1, 4, 7, 10, 14, 17, 21, 24, 27 and 31 d after urea addition). The incubation period for soil B was extended beyond 31 d to allow for additional data collection. On each sampling day, jars were opened for 5 min to allow equilibration of the headspace with lab air and then sealed. Jar headspace was manually sampled (10 mL) after 0, 30 and 60 min using a polypropylene syringe inserted through a rubber septum. Gas samples were transferred to glass vials that were analyzed within 96 h for N_2O using a gas chromatograph (model 5890, Agilent/Hewlett-Packard) equipped with a Porapak Q column, an electron capture detector and interfaced to an autosampler (model 7000, Teledyne Tekmar) (Maharjan and Venterea, 2013). The N_2O production rate was calculated from the rate of increase in N_2O concentration, headspace volume and dry soil mass. The jar contents were subsequently split into four subsamples. One (~5 g dry mass) subsample was immediately mixed with 38 mL 2 M KCl (pH = 12), shaken for 10 min and filtered for determination of $NO_2^- + NO_3^-$ (sum) and NO_2^- (by itself) using the Greiss–Ilosvay method with and without Cd reduction, respectively, in the same extract (Stevens and Laughlin, 1995; Mulvaney, 1996) using flow-through injection (Lachat, Loveland, CO) within 3–24 h of sampling. Concentrations of NO_3^- were calculated by difference. A second (~4 g dry mass) subsample was mixed with 38 mL 2 M KCl (pH = 5.6), shaken for 1 h and filtered for subsequent determination of total extractable ammonium (tNH_4^+). Extracts for tNH_4^+ were stored at 4 °C and analyzed using the sodium salicylate-nitroprusside method and flow-through injection (Mulvaney, 1996) within 7 d. A third (~2 g dry mass) subsample was mixed with 1 M KCl for soil pH determination. Soil pH was converted to H^+ concentrations (10^{-pH}) to facilitate intuitive data interpretation. A fourth (~1 g dry mass) subsample was transferred to a plastic vial and stored at −80 °C for subsequent DNA extraction and analysis which was performed on samples from nine of the 11 sampling dates (excluding days 24 and 27).

2.3. Quantitative polymerase chain reaction

Soil DNA was extracted from 0.25 g of previously frozen soil using a PowerSoil DNA isolation Kit (MoBio, Carlsbad, CA) in accordance with manufacturer protocol, except for the final washing step which was performed twice rather than once. Extraction yields were in the range of 10–30 ng DNA μL^{-1} quantified using a Qubit 2.0 Fluorometer (Thermo Fisher Scientific, Waltham, MA). Prior to the qPCR analyses, dilutions and reaction conditions were optimized for each gene. Following 10-fold dilution of extracts, 5 μL-aliquots were used for qPCR analyses using the 7500 Fast Real Time PCR system (Applied Biosystem, USA) and iTaq Universal SYBR Green Supermix (Bio-Rad, USA). All analyses were run in triplicate sets in 20-μL reaction mixtures containing 10 μL of SYBR Green supermix, 0.4 μM of primer and 5 μL of diluted template DNA in DNase free H_2O. The *amo*A, *nxr*A and *nxr*B genes were quantified using the primer pairs *amo*A-1F/*amo*A-2R (Rotthauwe et al., 1997), F1*nor*A/R2*nor*A (Wertz et al., 2008), and *nxr*B169f/*nxr*b638r (Pester et al., 2014), respectively. For *nxr*B, the master mix was supplemented with 1 μL of bovine serum albumin (20 μg μL^{-1}) and the annealing temperature was increased to 60 °C to improve primer specificity. The PCR conditions were as follows: 95 °C for 5 min and 35 cycles of 15 s at 95 °C for all three genes, followed by (i) for *amo*A, 30 s at 57 °C and 45 s at 72 °C, (ii) for *nxr*A, 30 s at 55 °C and 30 s at 72 °C, and (iii) for *nxr*B, 80 s at 60 °C, and, for all genes, followed by a dissociation phase from 60 to 95 °C to verify the melting curve of all samples. Gene copy numbers were determined with the standard curve method using gBlocks gene Fragments (Integrated DNA technology, USA). The R^2 values for all standard curves were ≥0.99 and primer efficiencies ranged from 80 to 95%. Gene copy number was expressed per gram of dry soil normalized to extraction yield of DNA (i.e., gene copies ng^{-1} DNA g^{-1} soil). In addition, the copy numbers of *nxr*A and *nxr*B were normalized to *amo*A copy numbers and are referred to here as the *nxr*A:*amo*A and *nxr*B:*amo*A ratios, respectively.

2.4. Ammonium sorption capacity (ASC) and ammonia determination

In parallel with the microcosm experiments, ASC was determined for each soil using batch isotherm methods. Preliminary trials were performed to determine optimum soil-to-solution ratios, solution concentrations and mixing times. Several solutions containing NH_4^+-N over the range of 0–500 μg N mL^{-1} were prepared using NH_4Cl in 0.01 M $CaCl_2$. Each solution (20 mL) was added to triplicate 50-mL polyethylene tubes containing 0.75 g of soil, which were then equilibrated on a reciprocating shaker at 100 rpm for 18 h followed by filtration and NH_4^+ analysis as described above. Sorbed ammonium ($srNH_4^+$) was plotted as the ordinate vs. the equilibrium solution-phase ammonium concentration ($slNH_4^+$) (Liu et al., 2008; Vogeler et al., 2011). The relationships for all soils were well described by a previously used ASC model (Venterea et al., 2015) (Supplementary Fig. S1):

$$srNH_4^+ = \frac{\mu\ slNH_4^+}{K + slNH_4^+} \quad (1)$$

The model parameters μ and K (Table 1) obtained by regression for each soil were used together with measured tNH_4^+ and pH to calculate corresponding solution-phase NH_3 concentrations in the microcosm experiment using equations developed by Venterea et al. (2015).

2.5. Data analysis

The microcosm experiments generated approximately 1000 values for each of 11 variables (H^+, NO_2^-, tNH_4^+, NH_3, N_2O, NO_3^-, *amo*A, *nxr*A, *nxr*B, *nxr*A:*amo*A and *nxr*B:*amo*A) producing ~12,000 total values. These variables are referred to as 'point-in-time' values to distinguish them from time-integrated, or 'cumulative,' values which were calculated by trapezoidal integration vs. time for each individual replicate microcosm (Burton et al., 2008; Venterea et al., 2015). This resulted in $n = 120$ for each cumulative variable. Cumulative variables are indicated by the prefix 'c-.' All variables, except c-H^+, were $\log_{10}$ transformed prior to analysis to meet the requirements of normality and homogeneity of variance, based on scatterplots of residuals vs. predicted values (Kutner et al., 2004) and the UNIVARIATE procedure of SAS (version 9.2, Cary, NC). Point-in-time and cumulative variables were each subjected to correlation analyses to determine if NO_2^- and N_2O were correlated with other variables, and single and multiple regression analyses with NO_2^- and N_2O as dependent variables and all other variables as independent variables using Statistix (version 9, Tallahassee, FL). Selected cumulative variables (c-NO_2^-, c-N_2O, c-NH_3, c-*amo*A, c-*nxr*A, c-*nxr*B) were analyzed by non-linear regression using individual replicate ($n = 15$) values for each soil type. Relationships between each variable and urea addition rate were evaluated for 10 regression models using the non-linear regression module in SigmaPlot (version 12.5, San Jose, CA), and two additional models (i.e., linear rise to maximum and linear decay to minimum) using the NLIN procedure of SAS. Cumulative variables were also analyzed at $P \leq 0.05$ using the MIXED procedure of SAS, with soil type and urea addition rate considered as fixed effects and replication and interactions with replication considered as random effects. Means were compared with pairwise t tests using the PDIFF option of the MIXED procedure of SAS.

3. Results

3.1. Point-in-time data

Point-in-time variables varied widely by soil type, urea addition rate, and over time (Supplementary Figs. S1 and S2). The time courses of the chemical variables during the first 10 d of incubation exhibited increases in pH and tNH_4^+, and thereafter exhibited decreases in pH and tNH_4^+, continual increases in NO_3^-, and transient increases in NO_2^- and N_2O. The time courses of gene abundances exhibited a variety of temporal patterns, tending to increase initially over the first 10–20 d, and then decrease, although there was substantial variation in these patterns by soil and urea addition rate. Compared to the treatments receiving urea, the control treatments exhibited little to no change in chemical variables except for some apparent increases in NO_3^-. Several significant correlations were evident among the point-in-time variables (Table 2). When accounting only for chemical variables, the strongest correlation was between NO_2^- and N_2O ($r = 0.78$), followed by NO_2^- and NH_3 ($r = 0.70$). With respect to gene abundances, NO_2^- and N_2O were both positively correlated with *amo*A gene copy number ($r = 0.66$ and 0.62, respectively), but were more strongly and negatively correlated with the *nxr*A:*amo*A ratio ($r = -0.79$ and −0.68, respectively).

The multiple linear regression model that explained the greatest amount of variance in NO_2^- included NH_3, and *amo*A and *nxr*A gene copy number as explanatory variables and accounted for 70% of the total variance (Fig. 1a). A model of the same structure, which included NH_3 together with the *nxr*A:*amo*A ratio as explanatory variables, also explained 70% of the variance. Substituting tNH_4^+ instead of NH_3 in these models resulted in a lower R^2 value (0.66).

Table 2
Pearson correlation coefficients (r) for chemical and genetic variables in microcosm experiments.[a]

Dependent variables	Independent variables										
	Chemical (concentrations)						Genetic (gene copy numbers)				
	Point-in-time ($n = 963$)										
	H^+	NH_4(t)	NH_3	NO_3	NO_2	N_2O	*amo*A	*nxr*A	*nxr*B	*nxr*A: *amo*A	*nxr*B: *amo*A
NO_2^-	−0.38	0.68	0.70	0.13	–	0.78	0.66	−0.16	ns[†]	−0.79	−0.60
N_2O	−0.10**[b]	0.59	0.47	0.29	0.78	–	0.62	ns	−0.10**	−0.68	−0.60
	Time-integrated ($n = 120$)										
	c-H^+	c-NH_4(t)	c-NH_3	c-NO_3	c-NO_2	c-N_2O	c-*amo*A	c-*nxr*A	c-*nxr*B	c-*nxr*A: c-*amo*A	c-*nxr*B: c-*amo*A
c-NO_2^-	−0.36	0.80	0.92	0.42	–	0.90	0.75	ns	ns	−0.88	−0.69
c-N_2O	−0.20*	0.81	0.81	0.46	0.90	–	0.76	ns	ns	−0.89	−0.74

[†]ns, not significant.
[a] All variables except c-H^+ were $\log_{10}$ transformed prior to analysis.
[b] Relationships for all r values shown are significant at $P < 0.001$, except when indicated by * ($P < 0.05$) or ** ($P < 0.01$).

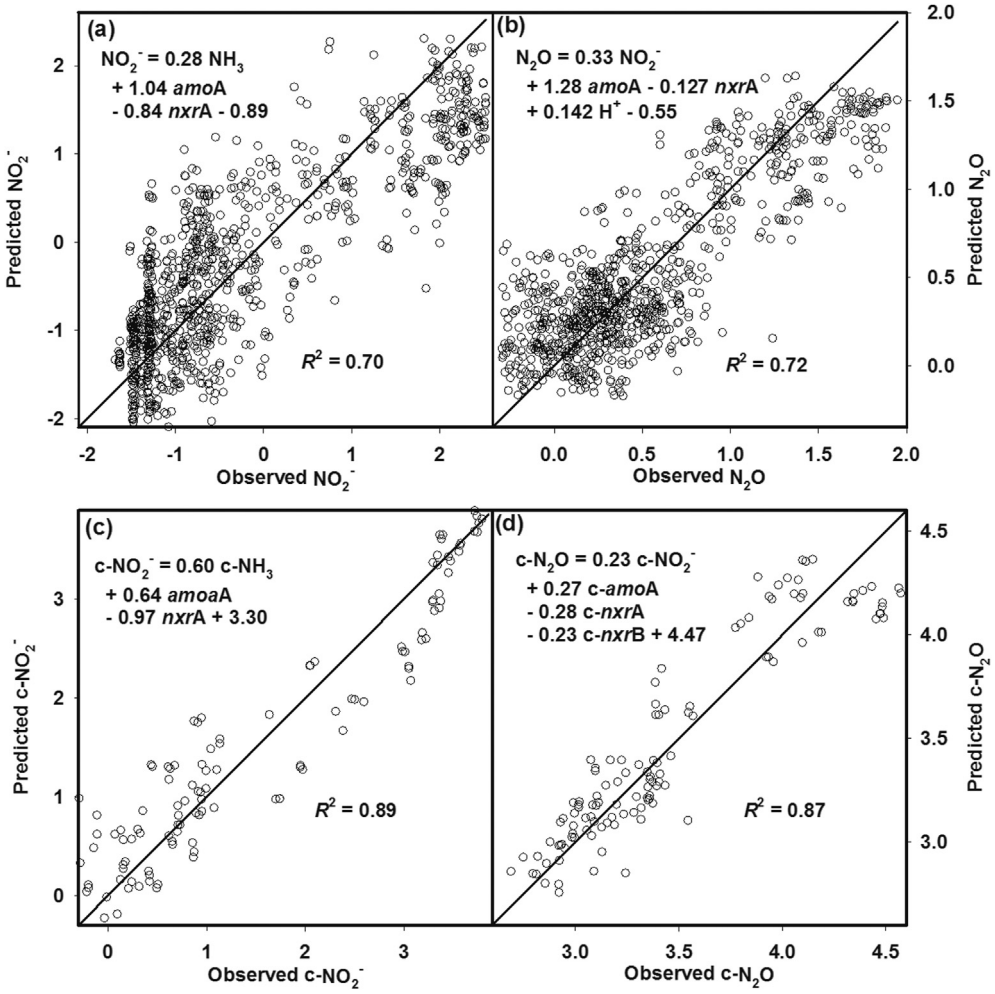

Fig. 1. Multiple regression models for (a) NO_2^-, (b) N_2O, (c) c-NO_2 and (d) c-N_2O. All variables were $\log_{10}$ transformed before analysis, and transformed data are shown. All explanatory variables were significant in models at $P < 0.001$. In (b), values of $N_2O < 0.5$ ng N g^{-1} h^{-1} were excluded from the model based on analysis of residuals (see section 3.1 for details).

A multiple regression model using a combination of chemical and genetic explanatory variables including NO_2^-, H^+, and *amo*A and *nxr*A gene copy numbers accounted for 66–72% of the variance in N_2O (Fig. 1b). Analysis of residuals indicated that observed N_2O values ≤ 0.5 ng N g^{-1} h^{-1} were consistently over-predicted by this model. When these low values ($n = 74$ or 7.6% of the data) were excluded, residuals were more normally distributed and the R^2 increased from 0.66 to 0.72. Separate analysis of the data for which $N_2O \leq 0.5$ ng N g^{-1} h^{-1} found no significant correlation with any chemical or genetic variables.

There were some significant ($P < 0.001$) correlations between basic soil properties and NO_2^-, but the relationships were weak, including pH ($r = 0.25$), organic matter ($r = -0.19$), clay ($r = -0.16$) and sand ($r = 0.15$) content. Silt ($r = -0.08$) and sand content ($r = 0.08$) were weakly correlated with N_2O ($P < 0.05$). Incubated soil water content was weakly correlated with NO_2^- ($r = -0.23$, $P < 0.001$) but not with N_2O. Including any of the basic soil properties with chemical and/or genetic variables did not improve the

amount of variance explained by the regression models for NO_2^- or N_2O.

3.2. Cumulative data

There was a significant ($P < 0.001$) soil-by-urea rate interaction for all cumulative variables (means separations in Tables S1–S3). Individual soil responses of c-NO_2^-, c-N_2O and c-NH_3 to urea addition rate were well described (R^2 = 0.89–0.99) by linear, exponential rise to maximum (ERM), exponential growth, sigmoidal and Gaussian peak models (Fig. 2, Table 3, Supplementary Table S4). For all soils except B, the same model type accurately described both the c-NO_2^- and c-N_2O responses. For soil B, the ERM model, which described the c-NO_2^- response, also described the c-N_2O response

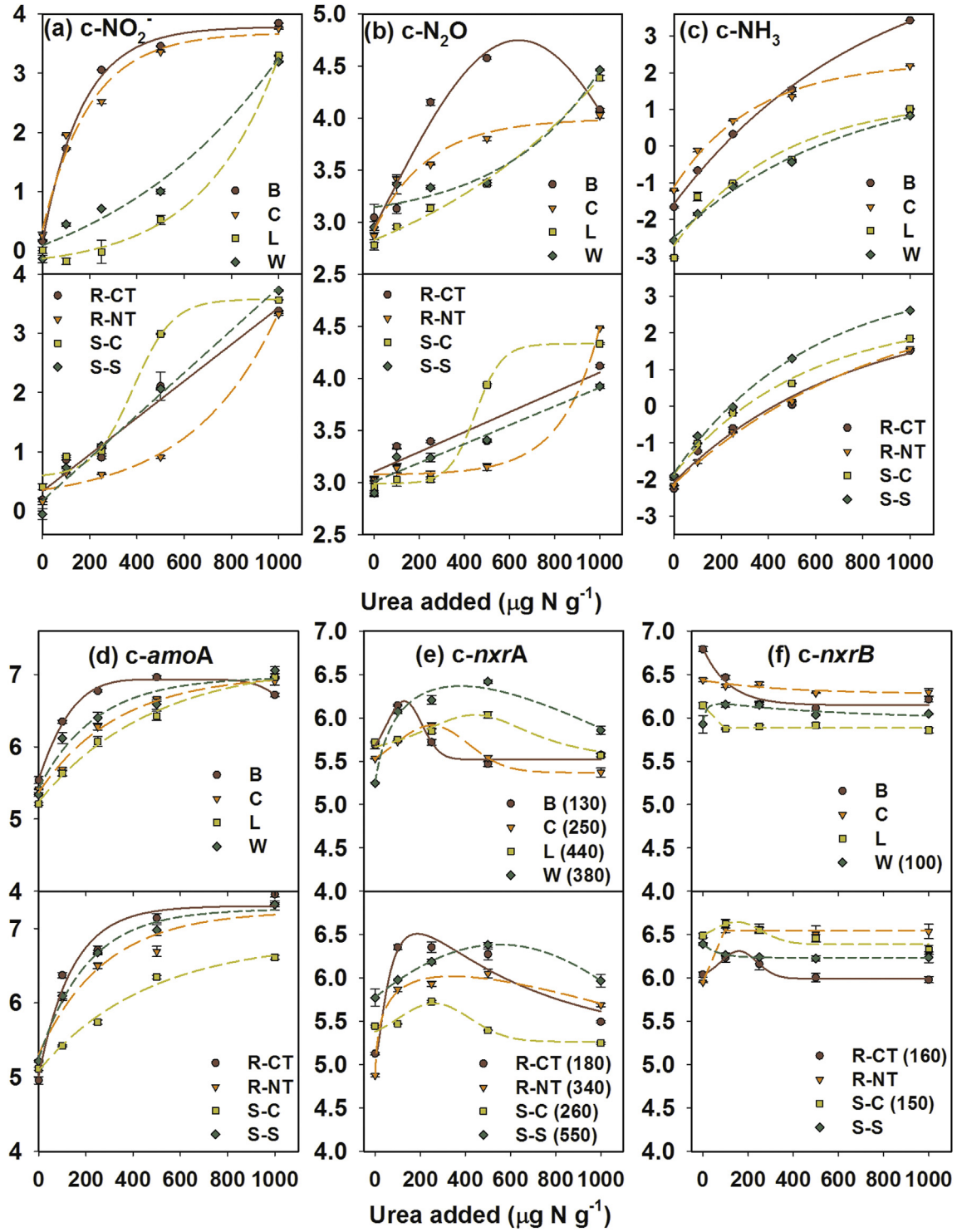

Fig. 2. Time-integrated (a) NO_2^-, (b) N_2O, (c) NH_3, (d) *amo*A, (e) *nxr*A and (f) *nxr*B at varying rates of urea addition to eight soils. Vertical axis variables are $\log_{10}$ transformed. Symbols are means with standard errors ($n = 3$) and lines are regression models (Table 3). In (e) and (f), values in parentheses are critical urea rates (U_c) corresponding to maximum *nxr*A or *nxr*B values for peak models.

Table 3
Regression models describing time-integrated chemical and genetic variables in soil microcosm experiments as a function of initial urea addition rate.[c]

Soil	Dependent variable[a]											
	c-NO_2^-		c-N_2O		c-NH_3		c-*amo*A		c-*nxr*A		c-*nxr*B	
	Model	R^2	Model	R^2	Model	R^2	Model	R^2	Model	R^2	Model	[b]R^2
B	ERM	0.99	GP3	0.92	ERM	0.99	GP3	0.99	GP4	0.95	ED	0.93
C	ERM	0.98	ERM	0.95	ERM	0.99	ERM	0.98	GP4	0.95	ED	0.61**
L	EG	0.98	EG	0.99	ERM	0.93	ERM	0.98	LP	0.90	LDM	0.87
W	EG	0.98	EG	0.92	ERM	0.99	ERM	0.93	WP	0.96	LogP	0.55*
R-CT	Lin	0.96	Lin	0.89	ERM	0.98	ERM	0.96	LogP	0.94	GP4	0.66**
R-NT	EG	0.98	EG	0.99	ERM	0.99	ERM	0.95	WP	0.98	LRM	0.87
S-C	Sig	0.99	Sig	0.98	ERM	0.99	ERM	0.99	GP4	0.92	GP4	0.63**
S-S	Lin	0.99	Lin	0.91	ERM	0.99	ERM	0.99	GP4	0.87	ED	0.63**

Model descriptions

Model	Equation
ED: Exponential decay	$y = y_0 + a^*\exp(-b^*x)$
EG: Exponential growth	$y = y_0 + a^*\exp(b^*x)$
ERM: Exponential rise to maximum	$y = y_0 + a^*[1 - \exp(-b^*x)]$
GP3: Gaussian peak, 3 parameter	$y = a^*\exp[-0.5^*[(x\text{-}x_0)/b]^2]$
GP4: Gaussian peak, 4 parameter	$y = y_0 + a^*\exp\{-0.5^*[(x\text{-}x_0)/b]^2\}$
Lin: Linear	$y = y_0 + a^*x$ for $x <$
LRM: Linear rise to maximum	$y = y_0 + a^*x$, *for* $x < x_0$; $y =$ b, *for* $x \geq x_0$; where $a > 0$
LDM: Linear decay to minimum	$y = y_0 + a^*x$, *for* $x < x_0$; $y =$ b, *for* $x \geq x_0$; where $a < 0$
LogP: Log-normal peak	$y = y_0 + (a/x)^*\exp[-0.5^*[\ln(x/x_0)/b]^2]$
LP: Lorentzian peak	$y = y_0 + a/\{1+[(x\text{-}x_0)/b]^2\}$
Sig: Sigmoidal	$y = y_0 + a/[1 + \exp(-(x\text{-}x_0)/b)]$
WP: Weibull peak	$y = a^*\Psi^{(1-c)/c}$ *abs$\{(x\text{-}x_0)/b + (\Psi^{1/c})^{c-1}\}$*exp{-abs$[(x\text{-}x_0)/b + (\Psi^{1/c})^c + \Psi]$}, where $\Psi=(c\text{-}1)/c$

[a] All dependent variables were $\log_{10}$ transformed prior to analysis.
[b] All models are significant at $P < 0.001$, except when indicated by * ($P < 0.05$) or ** ($P < 0.01$).
[c] Parameter values for all models are reported in Supplemental Table S4.

($R^2 = 0.91$, $P < 0.001$) but only when the highest urea addition rate (1000 μg N g^{-1}) was excluded. The ERM model described c-NH_3 for all soils ($R^2 \geq 0.93$).

The c-*amo*A gene abundances were well described by the ERM model ($R^2 = 0.93–0.99$) (Fig. 2d, Table 3) for all soils. In contrast, c-*nxr*A gene copy number was well described ($R^2 = 0.87–0.98$) for all soils by a 'peak' model, with the characteristic that c-*nxr*A gene copy number exhibited a maximum at intermediate urea addition rates (Fig. 2e, Table 3). The 'critical' urea addition rate (U_c), corresponding to the rate for which c-*nxr*A gene copy number was maximized, ranged from 130 to 550 μg N g^{-1} among soils (Fig. 2e).

The functional responses of c-*nxr*B gene abundance to urea addition were less consistent across soil types, compared to c-*nxr*A (Fig. 2f, Table 3). Whereas c-*nxr*A gene copy number for all soils were consistent with peak-type models, c-*nxr*B data were described by peak models for only three soils (W, R-CT and S-C), while variances for the remaining soils were more fully accounted for by exponential decay, linear decrease to minimum, and linear increase to maximum models. The selected models did not generally fit the c-*nxr*B data as well as the c-*nxr*A data as indicated by R^2 values. For three soils (B, L and S-S), c-*nxr*B was significantly less in the 100 μg N g^{-1} treatment compared to the control (0 μg N g^{-1}), while for four soils (W, R-CT, R-NT and S-C), c-*nxr*B was significantly greater in the 100 μg N g^{-1} treatment compared to the control (0 μg N g^{-1}) (Table S2).

Correlations among the time-integrated variables were similar to those observed for point-in-time variables, except that the relationships were stronger. Among the chemical variables, c-NO_2^- was strongly correlated with c-NH_3 ($r = 0.92$) and c-N_2O ($r = 0.90$) (Table 2). For genetic variables, c-NO_2^- and c-N_2O were positively correlated with c-*amo*A ($r = 0.75$ and 0.76, respectively), but were more strongly and negatively correlated with c-*nxr*A:c-*amo*A ($r = -0.88$ and -0.89, respectively). Considered as an explanatory variable, the c-*nxr*A:c-*amo*A ratio accounted for 78 and 79% of the variance in c-NO_2^- and c-N_2O, respectively (Fig. 3).

The multiple regression model that explained the greatest amount of variation in c-NO_2^- (89%) included c-NH_3, and the relative abundances of c-*amo*A and c-*nxr*A as explanatory variables (Fig. 1c), consistent with the results obtained for NO_2^-. A model of the same structure, which included c-NH_3 together with the c-*nxr*A:*amo*A ratio instead of c-*nxr*A and c-*amo*A gene copy numbers separately, explained 88% of the variance. Substituting c-tNH_4^+ instead of c-NH_3 in these models resulted in a lower R^2 value (0.79).

The multiple regression model that explained the greatest amount of variation in c-N_2O (87%) included NO_2^-, and abundances of *amo*A, *nxr*A and *nxr*B as explanatory variables (Fig. 1d). The form of this model was similar to that for N_2O (Fig. 1b), with the exceptions that c-*nxr*B gene copy number was also a significant ($P < 0.001$) explanatory variable and that including c-H^+ did not explain any additional variance in c-N_2O. Unlike the model for N_2O, there were no trends in residuals that varied with observed c-N_2O values.

There were some significant correlations between basic soil properties and c-NO_2^-, but the relationships were weak; e.g., pH ($r = 0.38$, $P < 0.001$), organic matter ($r = -0.29$, $P = 0.0012$), clay ($r = -0.22$, $P = 0.015$) and sand ($r = 0.21$, $P = 0.019$) content. Sand ($r = 0.22$) and silt content ($r = -0.19$) were weakly correlated with c-N_2O ($P < 0.05$). Incubated soil water content was weakly correlated with c-NO_2^- ($r = -0.34$, $P < 0.001$) and c-N_2O ($r = -0.19$, $P = 0.02$). Including any of the basic soil properties with chemical and/or genetic variables did not improve the multiple regression models for c-NO_2^- or c-N_2O.

4. Discussion

4.1. Variation in NO_2^- responses among soils

The soils examined here exhibited a wide range of NO_2^- responses to urea addition, and thus four different model types were required to describe them. Some soils showed much larger

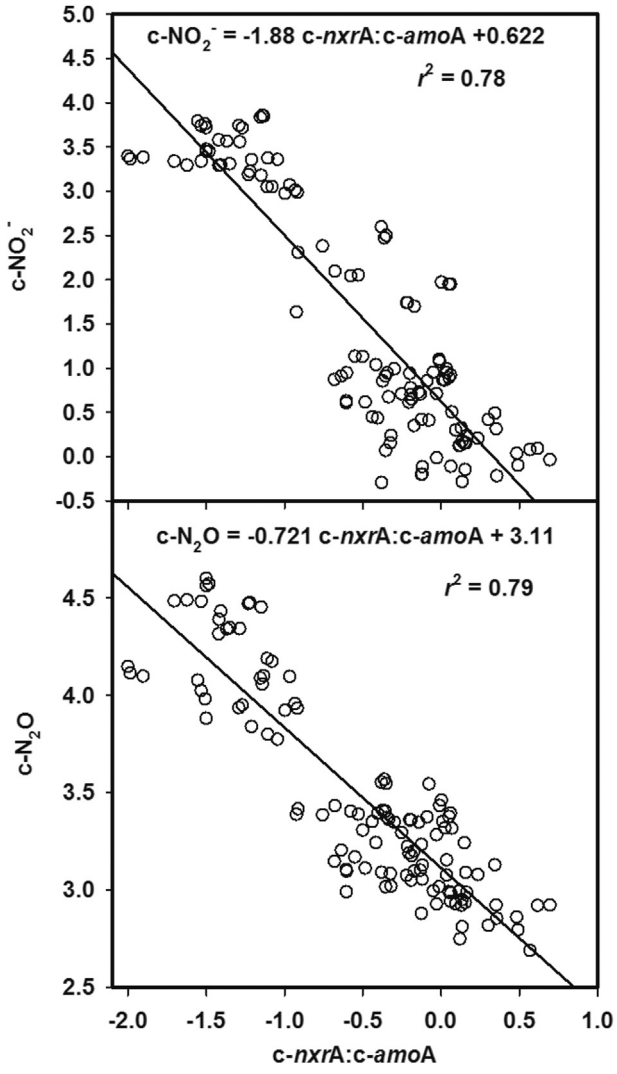

Fig. 3. Regression models describing (a) c-NO_2^- and (b) c-N_2O as a function of the c-*nxr*A:*amo*A ratio ($P < 0.001$). All variables were $\log_{10}$ transformed prior to analysis and transformed variables are plotted.

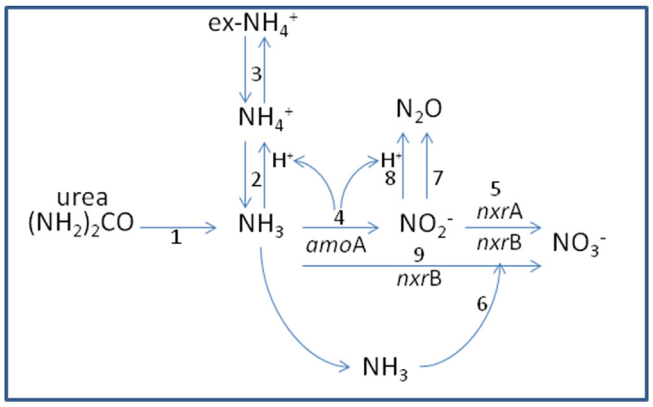

Fig. 4. Processes regulating NO_2^- accumulation and associated N_2O production following urea addition to soil. Urea hydrolysis (1) releases NH_3 which consumes H^+ in its equilibrium with NH_4^+ (2) while solution-phase NH_4^+ equilibrates (3) with exchangeable NH_4^+. NH_3 remaining in solution is oxidized (4) by AOB (*amo*A) to NO_2^- which also produces H^+. NO_2^- can be oxidized (5) by NOB (*nxr*A and *nxr*B) to NO_3^-. NH_3 can also inhibit (6) NOB resulting in accumulation of NO_2^- which promotes reduction (7) to N_2O via nitrifier-denitrification carried out by AOB, and chemo-denitrification (8) which may be enhanced by H^+. Also included is the possibility of complete nitrification from NH_3 to NO_3^- (9) carried out by some NOB within the genus *Nitrospira* (Daims et al., 2015; van Kessel et al., 2015).

responses at low to moderate urea addition rates. For example, following addition of 250 μg N g^{-1} urea, soils B and C exhibited 200- to 800-fold increases in c-NO_2^- compared to when no urea was added, while soils L, W and R-NT exhibited <10-fold increases in c-NO_2^-. In spite of the wide variation in individual soil responses, linear models with the same structure were able to describe NO_2^- and c-NO_2^- as a function of NH_3, and *amo*A and *nxr*A gene copy numbers across all soils and urea addition rates. These models are consistent with our understanding of the processes that affect NO_2^- accumulation under aerobic conditions, including urea hydrolysis, pH, and pH buffering capacity, NH_3 oxidation and ASC. Urea hydrolysis releases NH_3, which acts both as the primary substrate for AOB (*amo*A) that produce NO_2^- (Suzuki et al., 1974) and as an inhibitor of NOB (*nxr*A and *nxr*B) that utilize NO_2^- (Park and Bae, 2009). Thus, positive model coefficients for NH_3 and *amo*A gene copy number and the negative model coefficient for *nxr*A gene copy number are consistent with this description of key processes, as illustrated in Fig. 4.

Differences by soil type were not readily explained by basic soil properties ($|r| < 0.38$). This is not surprising given that NO_2^- dynamics are controlled by rates of both NH_3 and NO_2^- oxidation, and given the central role of free NH_3 concentrations which are influenced by multiple processes and properties. It is unlikely that all of these processes would be regulated by, or correlated with, any single soil property. Moreover, these findings demonstrate how it is possible for similar NH_3 and NO_2^- levels to evolve under contrasting initial soil conditions. This is illustrated by comparing the responses of soils B and C. Even though these two soils had contrasting pH, texture, CEC, and ASC (Table 1), they both accumulated greater NH_3 than all other soils (Fig. 2c), and had very similar NO_2^- responses to urea addition rate (Fig. 2a). The elevated NH_3 response in soil B was likely due to its low ACS, which was weakest of all soils. Weak ASC minimizes the removal of NH_4^+ from solution and thereby favors NH_3 formation during urea hydrolysis (Venterea et al., 2015). Whereas the ACS of soil C was approximately twice as strong as soil B, soil C also had the greatest initial pH and a strong buffering capacity as evidenced by relatively small changes in pH during incubation. Thus, even though soil C had lower solution-phase NH_4^+ than did soil B due to its greater ASC, the greater pH in soil C induced a greater fraction of the solution-phase NH_4^+ to disassociate to NH_3. Differences in nitrifier activity likely also contributed to the patterns in NH_3 and NO_2^- responses; e.g., soil B had greater c-*amo*A abundances than all soils except R-CT. These multiple differences and effects highlight the challenge of predicting NH_3, NO_2^- and N_2O based on static soil properties in a system driven by several interacting processes. Reports of NH_3 in soil N cycling studies are infrequent, and few studies have addressed its role in N_2O production. When it is quantified, NH_3 is typically determined based on measurements of tNH_4^+ and soil pH, together with the K_a value (e.g., Smith et al., 1997). While this simpler approach is valid in aqueous systems, in soils it ignores the role of sorption in regulating solution-phase NH_4^+ and NH_3.

4.2. Nitrite-mediated N_2O production

Given the oxic conditions maintained in the microcosms and the relatively weak correlation ($r = 0.29–0.46$) between NO_3^- and N_2O, heterotrophic denitrification was likely not an important process in this system. In contrast, the strong overall correlation ($r = 0.78–0.90$) between NO_2^- and N_2O indicate that nitrifier-

denitrification, and possibly chemo-denitrification, were the primary sources of N_2O given that these processes can reduce NO_2^- to N_2O under ambient as well as sub-ambient O_2 (Goreau et al., 1980; Wrage et al., 2001; Venterea, 2007). The positive coefficients for NO_2^- and *amo*A copy number, and negative coefficients for n*xr*B and/or *nxr*A copy number, in the regression models (Fig. 1b, d) are consistent with our understanding of N_2O production via nitrifier-denitrification; i.e., NO_2^- is the main substrate for AOB to produce N_2O, and when NOB abundances are reduced (e.g., due to NH_3 toxicity), NO_2^- becomes more readily available as a substrate for other reactions, among them the reduction to N_2O by AOB (Fig. 4). Although the *amo*A gene does not encode for N_2O production, its abundance is likely to be positively correlated with AOB abundances. The current results are also consistent with chemo-denitrification reactions between NO_2^- and soil organic matter that can produce N_2O under slightly acidic conditions (Stevenson et al., 1970; Thorn and Mikita, 2000). This mechanism is supported by the positive coefficient for H^+ in the model for N_2O (Fig. 1b), and by the finding that rate coefficients determined from the linear slope of the relationship between c-NO_2^- and c-N_2O for each soil were positively correlated ($r^2 = 0.63$, $P < 0.001$) with soil organic matter, consistent with Venterea (2007). However, when N_2O production was below 0.5 ng g^{-1} h^{-1} (<8% of the data) the regression model (Fig. 1b) over-predicted observed values, and there were no correlation between N_2O production and any measured variable. The majority of these data occurred in the control, where tNH_4^+ was <5 μg N g^{-1}. It is possible that AOA were important in producing N_2O under these low-substrate conditions, where AOA have been found to be more competitive than AOB (Prosser and Nicol, 2012). This hypothesis is consistent with a recent study that implicated the role of AOA in producing N_2O under low substrate conditions (Giguere et al., 2017).

4.3. Gene abundances

The c-*nxr*A abundances exhibited a consistent pattern of increasing and then decreasing below and above critical urea addition rates, respectively. This pattern is consistent with the hypothesis that *Nitrobacter*-associated NOB were inhibited by increasing levels of NH_3 (Figs. 2c and 3b). Under this hypothesis, soils with lower U_c values accumulate NO_2^- at lower urea addition rates. Indeed, for the majority of soils (six of eight), the contrasting NO_2^- responses shown in Fig. 2a were consistent with, and can be explained by, the differences in c-*nxr*A responses and U_c values. For example, soil S-C showed a steep increase in c-NO_2^- when urea was added at 500 μg N g^{-1} (Fig. 2a), and this coincided with a decline in *nxr*A (Fig. 2e). Also, the two soils (B and C) displaying the steepest increases in c-NO_2^- at urea addition rates ≤ 250 μg N g^{-1} also had U_c values ≤ 250 μg N g^{-1}, while the three soils (L, W and R-NT) with the least pronounced NO_2^- responses had U_c values ≥ 340 μg N g^{-1}. The c-NH_3 results are also consistent with these trends; soils B and C had greater c-NH_3 levels while soils L, W, and R-NT tended to have lower c-NH_3 (Fig. 2c). The c-NO_2^- results for the two soils (R-CT and S-S) that exhibited intermediate NO_2^- responses were not necessarily consistent with the above trends, which may have been due to inaccurate estimation of U_c as determined by the regression model. It is not surprising that *nxr*A by itself did not fully explain the NO_2^- responses, since NO_2^- must first be produced by AOB before it can accumulate, and it is logical that the abundances of NOB *relative to* AOB would be a better predictor of NO_2^- responses. In this sense, the *nxr*A:*amo*A gene copy ratio is actually a NO_2^- sink:source ratio, and as such, NO_2^- would be expected to increase as this ratio decreases. The *nxr*A:*amo*A ratio was the single best predictor of NO_2^-, a strong single predictor of N_2O and c-N_2O, and a significant predictor of NO_2^- and c-NO_2^- in the multiple regression models.

The contrasting responses of *nxr*A and *nxr*B abundances appear consistent with the greater affinity of *Nitrospira* (*nxr*B) relative to *Nitrobacter* (*nxr*A) for NO_2^- (Nowka et al., 2015). The abundances of *nxr*B were greater than *nxr*A in the control (no urea) treatments, where NO_2^- levels remained < 0.5 μg N g^{-1}. This trend is consistent with *Nitrospira* acting as a K-strategist wherein high population densities can be achieved despite substrate limitation. In contrast, the greater and more consistent increases in *nxr*A compared with *nxr*B abundances following urea addition are consistent with *Nitrobacter* being a r-strategist (Daims et al., 2016). These results are also in agreement with greater responsiveness of *Nitrobacter* (*nxr*A) relative to *Nitrospira* (*nxr*B) observed following N additions to soil (Simonin et al., 2015).

The consistency in the functional responses of *nxr*A abundances across soils, and the strong explanatory power of the c-*nxr*A:c-*amo*A ratio, suggest that *Nitrobacter* exerted greater regulatory control, in general, over NO_2^- and N_2O relative to *Nitrospira*. However, some differences in *nxr*B abundances among soils were observed, and may explain the corresponding differences in NO_2^- and N_2O. Most notable were the differences in *nxr*B gene copy number for soils R-CT and R-NT, which were sampled from long-term conventional tillage (CT) and no-till (NT) research plots, respectively. While the abundance of *nxr*B in R-CT exhibited a peak-type response indicative of NH_3 toxicity, abundances of this gene in R-NT showed no signs of suppression and were consistently greater than in R-CT except in the control (Fig. 2f). This finding suggests that greater activity of *Nitrospira* in R-NT was responsible for the significantly smaller NO_2^- and N_2O responses at intermediate urea addition rates as compared to R-CT (Fig. 2a and b). Moreover, this suggests that long-term implementation of NT caused shifts in dominant NOB populations such that *Nitrospira* under NT were able to maintain NO_2^- oxidizing activity in spite of similar NH_3 concentrations (Fig. 2c). It is possible that comammox capability within these *Nitrospira* populations resulted in a tighter coupling of the two steps of nitrification, due in large part to both processes being carried out by the same organism (Daims et al., 2015; van Kessel et al., 2015), although direct evidence of comammox occurring in agricultural soil has not been reported. In contrast to the greater abundance of *nxr*B in soil R-NT, a greater abundance of c-*amo*A was found in R-CT, except in the control (Table S2). The potential for shifts in dominant nitrifying populations due to tillage requires further investigation, but may be related to differences in soil organic matter, moisture retention and/or temperature (Venterea et al., 2006). Such shifts may also provide an explanation for the importance of long-term adoption of NT for effective N_2O mitigation (van Kessel et al., 2013).

Studies in wastewater found evidence for NH_3 inhibition of AOB (Park and Bae, 2009). Here, only soil B showed evidence of declining *amo*A abundances with increasing urea addition, and only at the highest addition rate (Fig. 2d). This decline in *amo*A abundances was consistent with NH_3 inhibition in that this treatment (soil B + 1000 μg N g^{-1}) had the greatest accumulation of NH_3 of any soil (Fig. 2c).

4.4. Conclusions and ecological implications

The wide variation in soil responses observed here could not be explained by basic soil properties. However, coherent models that incorporated N substrate concentrations and nitrification gene copy numbers accounted for 70–89% of the total variance in NO_2^- and N_2O. The time-integrated *nxr*A:*amo*A gene ratio was found to be a reliable sink:source ratio for NO_2^-, and explained 78 and 79% of the variance in cumulative NO_2^- and N_2O, respectively. In all soils, *nxr*A abundances declined above critical urea addition rates, indicating a consistent pattern of NH_3 suppression of *Nitrobacter*-

associated NOB. In contrast, *Nitrospira*-associated *nxr*B abundances exhibited a broader range of responses, and suggested that long-term management practices (e.g., tillage) can induce shifts in dominant NOB populations with impacts on NO_2^- accumulation and N_2O production. These results highlight the challenge of predicting NO_2^- and N_2O responses based solely on static soil properties in a system driven by dynamic and interacting physical, chemical, and biological processes, and suggest that models that account for the underlying processes are needed. In the field, a range of additional processes including fluctuating water content and temperature, plant N uptake and transport via advection and diffusion would likely reduce soil chemical concentrations and dampen the responses observed in these soil microcosms. The relationships found here provide a basis for incorporating the relevant chemical and biological processes into N cycling and N_2O emissions models that also account for these field-scale processes.

Acknowledgments

The authors gratefully acknowledge the assistance of Michael Dolan, Catherine Hastings and Christopher Staley. This work was supported in part by a grant from the Agricultural Fertilizer Research & Education Council of the Minnesota Department of Agriculture, contract no. 89688.

Appendix A. Supplementary data

Supplementary data related to this article can be found at http://dx.doi.org/10.1016/j.soilbio.2017.04.007.

References

Banning, N.C., Maccarone, L.D., Fisk, L.M., Murphy, D.V., 2015. Ammonia-oxidising bacteria not archaea dominate nitrification activity in semi-arid agricultural soil. Scientific Reports 5, 8.

Bertagnolli, A.D., McCalmont, D., Meinhardt, K.A., Fransen, S.C., Strand, S., Brown, S., Stahl, D.A., 2016. Agricultural land usage transforms nitrifier population ecology. Environmental Microbiology 18, 1918–1929.

Burns, L.C., Stevens, R.J., Laughlin, R.J., 1996. Production of nitrite in soil by simultaneous nitrification and denitrification. Soil Biology & Biochemistry 28, 609–616.

Burton, D.L., Li, X.H., Grant, C.A., 2008. Influence of fertilizer nitrogen source and management practice on N_2O emissions from two Black Chernozemic soils. Canadian Journal of Soil Science 88, 219–227.

Cai, Z., Gao, S., Hendratna, A., Duan, Y., Xu, M., Hanson, B.D., 2016. Key factors, soil nitrogen processes, and nitrite accumulation affecting nitrous oxide emissions. Soil Science Society of America Journal 80, 1560–1571.

Chen, Y.L., Xu, Z.W., Hu, H.W., Hu, Y.J., Hao, Z.P., Jiang, Y., Chen, B.D., 2013. Responses of ammonia-oxidizing bacteria and archaea to nitrogen fertilization and precipitation increment in a typical temperate steppe in Inner Mongolia. Applied Soil Ecology 68, 36–45.

Ciais, P., Sabine, C., Bala, G., Bopp, L., Brovkin, V., Canadell, J., Chhabra, A., DeFries, R., Galloway, J., Heimann, M., Jones, C., Quéré, C.L., Myneni, R.B., Piao, S., Thornton, P., 2013. Carbon and other biogeochemical cycles. In: Stocker, T.F., Qin, D., Plattner, G.-K., Tignor, M., Allen, S.K., Boschung, J., Nauels, A., Xia, Y., Bex, V., Midgley, P.M. (Eds.), Climate Change 2013: the Physical Science Basis. Contribution of Working Group I to the Fifth Assessment Report of the Intergovernmental Panel on Climate Change. Cambridge University Press, New York, NY, pp. 465–570.

Crutzen, P.J., Mosier, A.R., Smith, K.A., Winiwarter, W., 2008. N2O release from agro-biofuel production negates global warming reduction by replacing fossil fuels. Atmospheric Chemistry and Physics 8, 389–395.

Daims, H., Lebedeva, E.V., Pjevac, P., Han, P., Herbold, C., Albertsen, M., Jehmlich, N., Palatinszky, M., Vierheilig, J., Bulaev, A., Kirkegaard, R.H., von Bergen, M., Rattei, T., Bendinger, B., Nielsen, P.H., Wagner, M., 2015. Complete nitrification by *Nitrospira* bacteria. Nature 528, 504–509.

Daims, H., Lucker, S., Wagner, M., 2016. A new perspective on microbes formerly known as nitrite-oxidizing bacteria. Trends in Microbiology 24, 699–712.

Davidson, E.A., 2009. The contribution of manure and fertilizer nitrogen to atmospheric nitrous oxide since 1860. Nature Geoscience 2, 659–662.

Di, H.J., Cameron, K.C., Shen, J.P., Winefield, C.S., O'Callaghan, M., Bowatte, S., He, J.Z., 2009. Nitrification driven by bacteria and not archaea in nitrogen-rich grassland soils. Nature Geoscience 2, 621–624.

Firestone, M.K., Davidson, E.A., 1989. Microbiological basis of NO and N2O production and consumption in soil. In: Andreae, M.O., Schimel, D.S. (Eds.), Exchange of Trace Gases between Terrstrial Ecosystems and the Atmosphere. John Wiley & Sons Ltd, New York, pp. 7–21.

Forster, P., Ramaswamy, V., Artaxo, P., Berntsen, T., Betts, R., Fahey, D.W., Haywood, J., Lean, J., Lowe, D.C., Myhre, G., Nganga, J., Prinn, R., Raga, G., Schultz, M., Van Dorland, R., 2007. In: Solomon, S., Qin, D., Manning, M., Chen, Z., Marquis, M., Averyt, K.B., Tignor, M., Miller, H.L. (Eds.), Changes in Atmospheric Constituents and in Radiative Forcing. Cambridge University Press, Cambridge, United Kingdom, pp. 129–234.

Giguere, A.T., Taylor, A.E., Myrold, D.D., Bottomley, P.J., 2015. Nitrification responses of soil ammonia-oxidizing archaea and bacteria to ammonium concentrations. Soil Science Society of America Journal 79, 1366–1374.

Giguere, A.T., Taylor, A.E., Suwa, Y., Myrold, D.D., Bottomley, P.J., 2017. Uncoupling of ammonia oxidation from nitrite oxidation: impact upon nitrous oxide production in non-cropped Oregon soils. Soil Biology & Biochemistry 104, 30–38.

Goreau, T.J., Kaplan, W.A., Wofsy, S.C., Mcelroy, M.B., Valois, F.W., Watson, S.W., 1980. Production of NO_2^- and N_2O by nitrifying bacteria at reduced concentrations of oxygen. Applied and Environmental Microbiology 40, 526–532.

Heil, J., Vereecken, H., Bruggemann, N., 2016. A review of chemical reactions of nitrification intermediates and their role in nitrogen cycling and nitrogen trace gas formation in soil. European Journal of Soil Science 67, 23–39.

Homyak, P.M., Vasquez, K.T., Sickman, J.O., Parker, D.R., Schimel, J.P., 2015. Improving nitrite analysis in soils: drawbacks of the conventional 2 M KCl extraction. Soil Science Society of America Journal 79, 1237–1242.

Kelly, J.J., Policht, K., Grancharova, T., Hundal, L.S., 2011. Distinct responses in ammonia-oxidizing archaea and bacteria after addition of biosolids to an agricultural soil. Applied and Environmental Microbiology 77, 6551–6558.

Koch, H., Lucker, S., Albertsen, M., Kitzinger, K., Herbold, C., Spieck, E., Nielsen, P.H., Wagner, M., Daims, H., 2015. Expanded metabolic versatility of ubiquitous nitrite-oxidizing bacteria from the genus *Nitrospira*. Proceedings of the National Academy of Sciences of the United States of America 112, 11371–11376.

Kutner, M.H., Nachtsheim, C.J., Neter, J., 2004. Applied Linear Regression Models, 4 ed. McGraw-Hill, New York.

Liu, Y.L., Zhang, B., Li, C.L., Hu, F., Velde, B., 2008. Long-term fertilization influences on clay mineral composition and ammonium adsorption in a rice paddy soil. Soil Science Society of America Journal 72, 1580–1590.

Ma, L., Shan, J., Yan, X.Y., 2015. Nitrite behavior accounts for the nitrous oxide peaks following fertilization in a fluvo-aquic soil. Biology and Fertility of Soils 51, 563–572.

Maharjan, B., Venterea, R.T., 2013. Nitrite intensity explains N management effects on N_2O emissions in maize. Soil Biology & Biochemistry 66, 229–238.

Mulvaney, R.L., 1996. Nitrogen-inorganic forms. In: Sparks, D.L. (Ed.), Methods of Soil Analysis. Am. Soc. Agron., Madison, WI, pp. 1123–1184.

Nowka, B., Daims, H., Spieck, E., 2015. Comparison of oxidation kinetics of nitrite-oxidizing bacteria: nitrite availability as a key factor in niche differentiation. Applied and Environmental Microbiology 81, 745–753.

Park, S., Bae, W., 2009. Modeling kinetics of ammonium oxidation and nitrite oxidation under simultaneous inhibition by free ammonia and free nitrous acid. Process Biochemistry 44, 631–640.

Pester, M., Maixner, F., Berry, D., Rattei, T., Koch, H., Lucker, S., Nowka, B., Richter, A., Spieck, E., Lebedeva, E., Loy, A., Wagner, M., Daims, H., 2014. *nxr*B encoding the beta subunit of nitrite oxidoreductase as functional and phylogenetic marker for nitrite-oxidizing *Nitrospira*. Environmental Microbiology 16, 3055–3071.

Prosser, J.I., Nicol, G.W., 2012. Archaeal and bacterial ammonia-oxidisers in soil: the quest for niche specialisation and differentiation. Trends in Microbiology 20, 523–531.

Ravishankara, A.R., Daniel, J.S., Portmann, R.W., 2009. Nitrous oxide (N_2O): the dominant ozone-depleting substance emitted in the 21st century. Science 326, 123–125.

Robertson, G.P., Vitousek, P.M., 2009. Nitrogen in agriculture: balancing the cost of an essential resource. Annual Review of Environment and Resources 34, 97–125.

Rotthauwe, J.H., Witzel, K.P., Liesack, W., 1997. The ammonia monooxygenase structural gene *amo*A as a functional marker: molecular fine-scale analysis of natural ammonia-oxidizing populations. Applied and Environmental Microbiology 63, 4704–4712.

Schauss, K., Focks, A., Leininger, S., Kotzerke, A., Heuer, H., Thiele-Bruhn, S., Sharma, S., Wilke, B.M., Matthies, M., Smalla, K., Munch, J.C., Amelung, W., Kaupenjohann, M., Schloter, M., Schleper, C., 2009. Dynamics and functional relevance of ammonia-oxidizing archaea in two agricultural soils. Environmental Microbiology 11, 446–456.

Shcherbak, I., Millar, N., Robertson, G.P., 2014. Global metaanalysis of the nonlinear response of soil nitrous oxide (N_2O) emissions to fertilizer nitrogen. Proceedings of the National Academy of Sciences of the United States of America 111, 9199–9204.

Shen, J.P., Zhang, L.M., Di, H.J., He, J.Z., 2012. A review of ammonia-oxidizing bacteria and archaea in Chinese soils. Frontiers in Microbiology 3, 7.

Shen, Q.R., Ran, W., Cao, Z.H., 2003. Mechanisms of nitrite accumulation occurring in soil nitrification. Chemosphere 50, 747–753.

Simonin, M., Le Roux, X., Poly, F., Lerondelle, C., Hungate, B.A., Nunan, N., Niboyet, A., 2015. Coupling between and among ammonia oxidizers and nitrite oxidizers in grassland mesocosms submitted to elevated CO_2 and nitrogen supply. Microbial Ecology 70, 809–818.

Smith, R.V., Doyle, R.M., Burns, L.C., Stevens, R.J., 1997. A model for nitrite accumulation in soils. Soil Biology & Biochemistry 29, 1241–1247.

Sterngren, A.E., Hallin, S., Bengtson, P., 2015. Archaeal ammonia oxidizers dominate

in numbers, but bacteria drive gross nitrification in N-amended grassland soil. Frontiers in Microbiology 6.
Stevens, R.J., Laughlin, R.J., 1995. Nitrite transformations during soil extraction with potassium-chloride. Soil Science Society of America Journal 59, 933–938.
Stevenson, F.J., Harrison, R.M., Wetselaar, R., Leeper, R.A., 1970. Nitrosation of soil organic matter: III. Nature of gases produced by reaction of nitrite with lignins, humic substances, and phenolic constituents under neutral and slightly acidic conditions. Soil Science Society of America Journal 34, 430–435.
Stojanovic, B.J., Alexander, M., 1958. Effect of inorganic nitrogen on nitrification. Soil Science 86, 208–215.
Suzuki, I., Dular, U., Kwok, S.C., 1974. Ammonia or ammonium ion as substrate for oxidation by *Nitrosomonas europaea* cells and extracts. Journal of Bacteriology 120, 556–558.
Thorn, K.A., Mikita, M.A., 2000. Nitrite fixation by humic substances: nitrogen-15 nuclear magnetic resonance evidence for potential intermediates in chemo-denitrification. Soil Science Society of America Journal 64, 568–582.
Van Cleemput, O., Samater, A.H., 1995. Nitrite in soils: accumulation and role in the formation of gaseous N compounds. Fertilizer Research 45, 81–89.
van Kessel, C., Venterea, R., Six, J., Adviento-Borbe, M.A., Linquist, B., van Groenigen, K.J., 2013. Climate, duration, and N placement determine N2O emissions in reduced tillage systems: a meta-analysis. Global Change Biology 19, 33–44.
van Kessel, M.A.H.J., Speth, D.R., Albertsen, M., Nielsen, P.H., Op den Camp, H.J.M., Kartal, B., Jetten, M.S.M., Lücker, S., 2015. Complete nitrification by a single microorganism. Nature 528, 555–559.
Venterea, R.T., 2007. Nitrite-driven nitrous oxide production under aerobic soil conditions: kinetics and biochemical controls. Global Change Biology 13, 1798–1809.
Venterea, R.T., Baker, J.M., Dolan, M.S., Spokas, K.A., 2006. Carbon and nitrogen storage are greater under biennial tillage in a Minnesota corn-soybean rotation. Soil Science Society of America Journal 70, 1752–1762.
Venterea, R.T., Clough, T.J., Coulter, J.A., Breuillin-Sessoms, F., Wang, P., Sadowsky, M.J., 2015. Ammonium sorption and ammonia inhibition of nitrite-oxidizing bacteria explain contrasting soil N_2O production. Scientific Reports 5, 12153.
Venterea, R.T., Halvorson, A.D., Kitchen, N., Liebig, M.A., Cavigelli, M.A., Del Grosso, S.J., Motavalli, P.P., Nelson, K.A., Spokas, K.A., Singh, B.P., Stewart, C.E., Ranaivoson, A., Strock, J., Collins, H., 2012. Challenges and opportunities for mitigating nitrous oxide emissions from fertilized cropping systems. Frontiers in Ecology and the Environment 10, 562–570.
Venterea, R.T., Rolston, D.E., 2000. Nitric and nitrous oxide emissions following fertilizer application to agricultural soil: biotic and abiotic mechanisms and kinetics. Journal of Geophysical Research-atmospheres 105, 15117–15129.
Vogeler, I., Cichota, R., Snow, V.O., Dutton, T., Daly, B., 2011. Pedotransfer functions for estimating ammonium adsorption in soils. Soil Science Society of America Journal 75, 324–331.
Wang, F., Bear, J., Shaviv, A., 1998. Modelling simultaneous release, diffusion and nitrification of ammonium in the soil surrounding a granule or nest containing ammonium fertilizer. European Journal of Soil Science 49, 351–364.
Wang, Q., Zhang, L.M., Shen, J.P., Du, S., Han, L.L., He, J.Z., 2016. Nitrogen fertiliser-induced changes in N2O emissions are attributed more to ammonia-oxidising bacteria rather than archaea as revealed using 1-octyne and acetylene inhibitors in two arable soils. Biology and Fertility of Soils 52, 1163–1171.
Wertz, S., Leigh, A.K.K., Grayston, S.J., 2012. Effects of long-term fertilization of forest soils on potential nitrification and on the abundance and community structure of ammonia oxidizers and nitrite oxidizers. Fems Microbiology Ecology 79, 142–154.
Wertz, S., Poly, F., Le Roux, X., Degrange, E., 2008. Development and application of a PCR-denaturing gradient gel electrophoresis tool to study the diversity of Nitrobacter-like nxrA sequences in soil. Fems Microbiology Ecology 63, 261–271.
Wetselaar, R., Passioura, J.B., Singh, B.R., 1972. Consequences of banding nitrogen fertilizers in soil. I. Effects on nitrification. Plant and Soil 36, 159–175.
Wrage, N., Velthof, G.L., van Beusichem, M.L., Oenema, O., 2001. Role of nitrifier denitrification in the production of nitrous oxide. Soil Biology & Biochemistry 33, 1723–1732.
Yadvinder-Singh, Beauchamp, E.G., 1989. Nitrogen transformations near urea in soil: effects of nitrification inhibition, nitrifier activity and liming. Fertilizer Research 18, 201–212.
Zhang, L.M., Hu, H.W., Shen, J.P., He, J.Z., 2012. Ammonia-oxidizing archaea have more important role than ammonia-oxidizing bacteria in ammonia oxidation of strongly acidic soils. Isme Journal 6, 1032–1045.
Zhou, F., Shang, Z.Y., Zeng, Z.Z., Piao, S.L., Ciais, P., Raymond, P.A., Wang, X.H., Wang, R., Chen, M.P., Yang, C.L., Tao, S., Zhao, Y., Meng, Q., Gao, S.S., Mao, Q., 2015. New model for capturing the variations of fertilizer-induced emission factors of N_2O. Global Biogeochemical Cycles 29, 885–897.
Zumft, W.G., 1997. Cell biology and molecular basis of denitrification. Microbiology and Molecular Biology Reviews 61, 533–616.